Chapter 9

MAFIC INTRUSIONS

9.1 Introduction

These are intrusive into the Archaean Manica Greenstone Belt and Vumba Granite Gneiss in the west, and the Early and Late Proterozoic Messica Granite Gneiss and Nhansipfe Granitic Orthogneiss in the east respectively. Those in the E commonly form dykes (Fig. 2.1). The intrusions forming dykes in both E and W areas are oriented ~N-S and are, therefore, considered to be coeval. The N-S orientation is similar to the Umkondo Group sills in SE Zimbabwe which are dated at ~1080 Ma old (Allsop *et al.*, 1989). The lack of a strong deformational fabric, typical of the Mozambique Metamorphic Province, in the mafic rocks of the study area suggests that these might not be that old. This assessment could find some support from Pinna *et al.*(1986) who indicated an age of between ~500-~1100 Ma for some post-Umkondo mafic intrusions.

9.2 Field Description

The mafic rocks are intrusive into both the Archaean Zimbabwe Craton and the Proterozoic Mozambique Metamorphic Province, occurring mostly as dykes in the latter (Fig. 2.1). They vary from gabbros to dolerites and have a similar mineralogical composition characterized by white plagioclase, greenish and stubby clinopyroxene grains and black short prismatic to acicular amphibole grains. They are commonly chloritized, suggesting metamorphism under greenschist facies conditions, and are inequigranular medium-grained. Mafic intrusions within the Mozambique Metamorphic Province, unlike those within the Craton, commonly occur as dykes with N-S orientations and intrude both the granitoids and the metasediments. They are represented by amphibolitic dolerites. They were studied in Garuzo, Chicamba, Mombeza and Vanduzi areas (Figure 2.2). Mineralogically two groups are distinguishable, namely, one in which the mineral assemblage, is dominated by plagioclase, hornblende, pyroxene, quartz, and garnet, and which has a granoblastic metamorphic texture and another group which is characterized by the absence of garnet and relict igneous textures. The former occurs E of the Messica area and the latter to the west. The amphibolites occur as dykes of fine- to medium-grained rocks in the Garuzo, Chicamba, Vanduzi and Mombeza areas (Figure2.2). The foliation in the amphibolite is defined by the preferred orientation of inequant minerals that include hornblende and deformed plagioclase and quartz. Migmatization in amphibolite also took place as is shown in Figure 9.1 in which the migmatization is indicated by planar quartzo-feldspathic leucosomes in an amphibolite dyke intruding a porphyritic foliated granite. The fact that the partial melt patches are parallel to the N-S foliation suggests their development during the second phase of deformation (the first produced a E-W foliation and predates the amphibolite intrusion).

Figure 9.1: Patches of partial melts in the amphibolite intruding a megacrystic granite.

9.3 Petrography

The mineralogy of these rocks is shown in Table 9.1. Two groups of rocks are represented, namely, one with typical igneous ophitic texture and another with metamorphic granoblastic textures.

Table 9.1: Mineral assemblage of mafic rocks. Numbers represent mineral proportions.

sample	Plg	Amp	Cpx	Opx	Qtz	Grt	Chl	Ep	Ttn	Opm	texture
18S	45	40	7	-	-	-	2	1	1	4	igneous
MDo	45	42	5	-	-	-	5	1	-	2	igneous
15M	37	39	15	-	-	-	3	1	-	5	igneous
12T	52	10	30	-	-	-	1	1	1	5	igneous
maamp1	20	60	10	-	1	5	-	-	2	2	metam
maamp	25	56	8	-	1	5	-	-	2	2	metam
maamp2	15	75	1	-	1	-	-	-	5	3	metam
amp*	18	65	8	-	-	-	-	-	8	1	metam
mramp	45	35	4	1	2	8	-	-	3	2	metam
chm	33	62	-	-	2	-	-	-	1	2	metam
mbamp	34	44	8	2	2	5	-	-	3	2	metam

Plg- plagioclase, Amp- amphibole, Cpx- clinopyroxene, Opx- Orthopyroxene, Qtz- quartz, Grt- garnet, Chl- chlorite, Ep- epidote, Ttn- titanite and Opm- opaque minerals; metam- metamorphic.

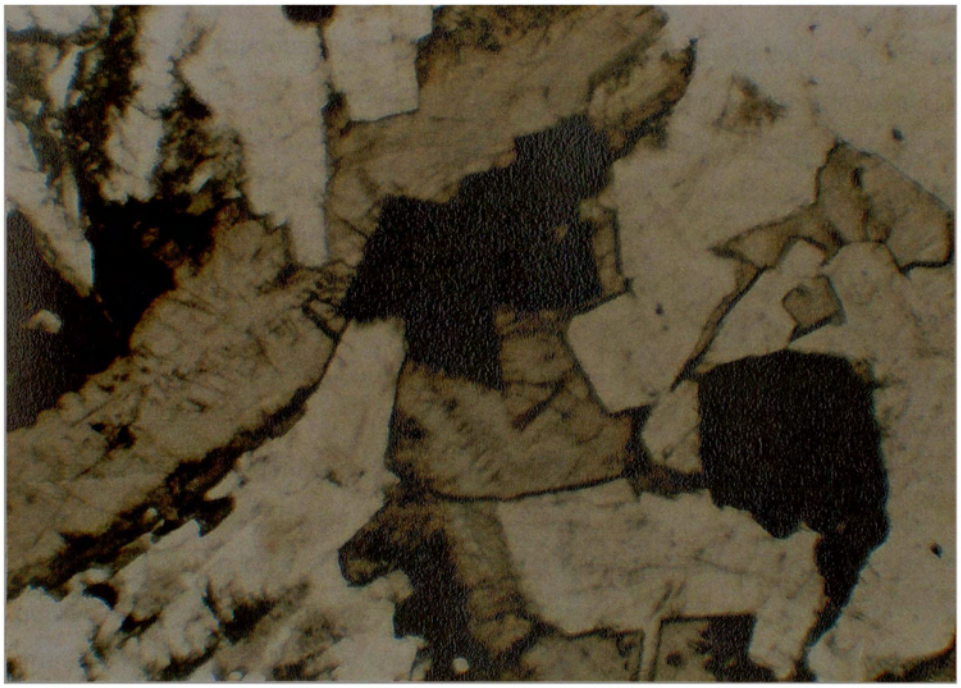

Figure 9.2: Clinopyroxene (brown), plagioclase (white), chlorite (greenish), amphibole (green, top left) and opaque minerals (black) of the igneous mafic rocks. Parallel light, width of field 7 mm.

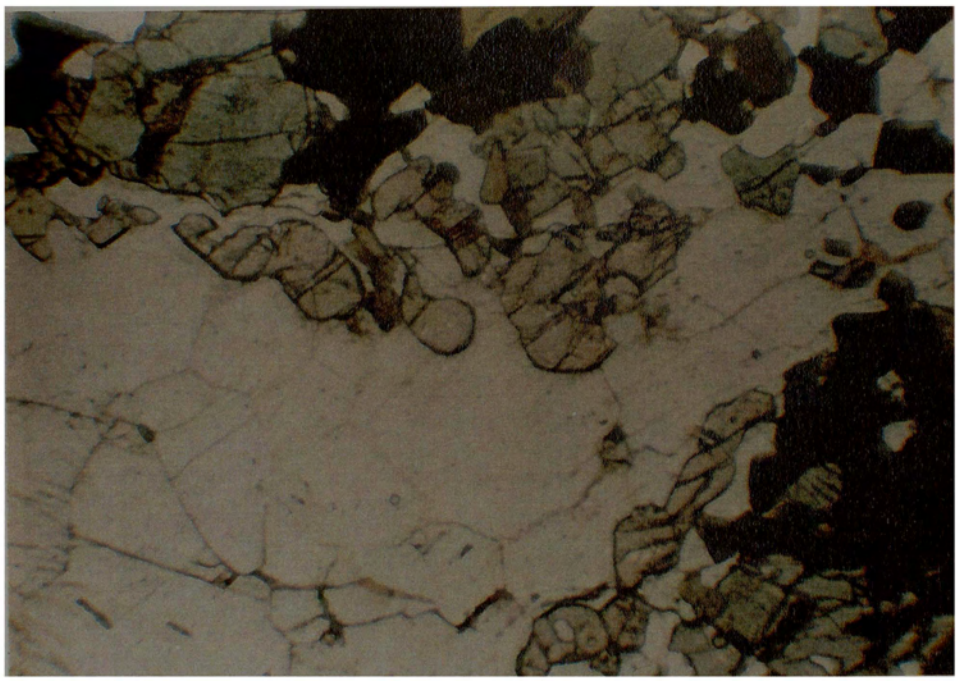

Figure 9.3: Granoblastic-polygonal texture showing plagioclase (white) with 120° triple junctions, adjoining amphibole (green) and xenoblastic garnet (light brown, included in plagioclase) and opaque minerals (black). Parallel light, width of field 7 mm.

In general the igneous rocks are fine- to medium-grained with the ferromagnesian minerals occupying spaces between plagioclase grains (Fig. 9.2) whereas the dominant texture in the metamorphic rocks is granoblastic because of textural re-equilibration (Shelley, 1993, p. 104) (Fig. 9.3).

The mineralogy of these mafic rocks is dominated by plagioclase and amphibole whereas garnet occurs in the metamorphosed equivalents.

The samples are characterized by saussuritization of plagioclase, and chloritization and uralitization of clinopyroxene. Plagioclase is commonly zoned and either represents magmatic disequilibrium during emplacement or disequilibrium during partial metamorphic hydration. The dominant amphibole is actinolite in the rocks with igneous textures and hornblende in the metamorphic rocks whereas pyroxene is represented by clinopyroxene. Small proportions of orthopyroxene and quartz occur in some metamorphic samples.

In samples with igneous textures plagioclase is saussuritized, sericitized and contains inclusions of garnet. Amphibole occurs as idiomorphic to lobate xenomorphic and needle-like grains, some of which are altered to chlorite and enclose grains of plagioclase, epidote and opaque minerals. Pyroxene occurs as euhedral to subhedral grains which commonly show zoning, weak pleochroism and simple twinning. At the grain boundaries some grains are altered to chlorite (Fig. 9.2). Locally it contains small inclusions of plagioclase and appears also as relict grains in rocks where the predominant ferromagnesian mineral is amphibole. Epidote is a minor, but important component and is generally associated with plagioclase in which it occurs as inclusions, as an alteration product. Titanite and opaque minerals accessories and are commonly associated with ferromagnesian silicates.

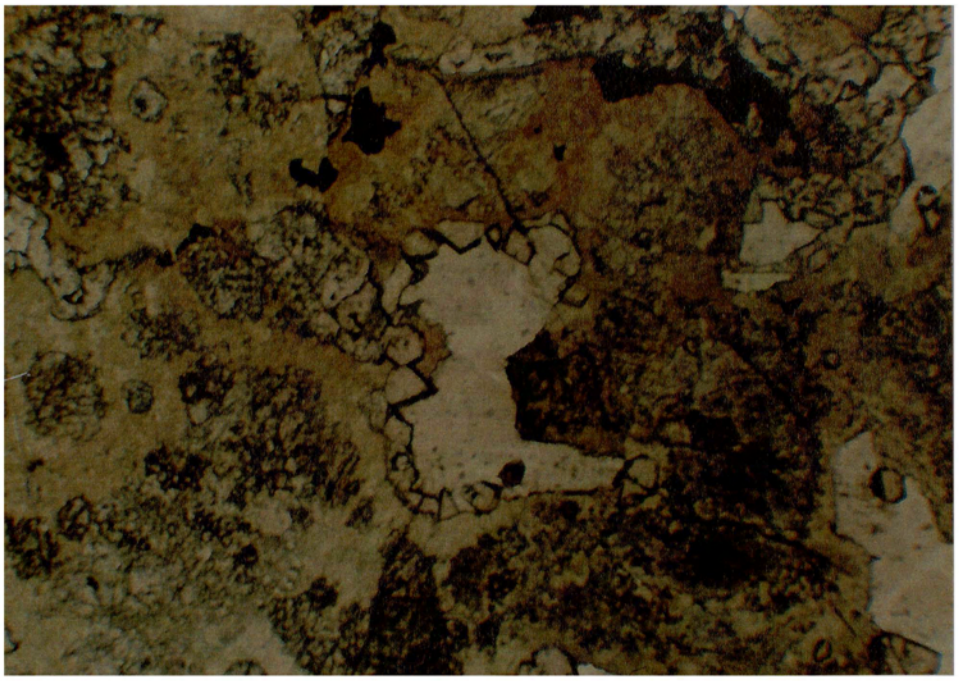

Figure 9.4: Idioblastic fine grained garnet (high relief) associated with both plagioclase (white) and amphibole (green) in the metamorphosed mafic rocks. Parallel light, width of field 7 mm.

Figure 9.5: Xenoblastic grains of garnet with symplectitic inclusions of plagioclase. Parallel light width of field 3 mm.

In the metamorphic rocks plagioclase occurs as sub-idiomorphic rectangular and equant grains exhibiting typical plagioclase twinning. In general the laths are fresh in appearance whereas the equant grains are locally saussuritized, sericitized cracked and filled with inclusions. Amphibole occurs as large grains with irregular faces enclosing finer grains of plagioclase as well as quartz or as equant grains normally showing granoblastic texture. Locally amphibole is altered to chlorite. Clinopyroxene is commonly weakly pleochroic and occurs as brown to reddish brown equant anhedral grains. Rare orthopyroxene is brown, pleochroic and exhibits straight extinction. Garnet occurs as fine-grained idiomorphic grains, commonly associated with plagioclase and amphibole and as coarser xenoblastic grains which contain inclusions of fine plagioclase and, rarely, amphibole and pyroxene grains (Figs. 9.4 and 9.5). Quartz is strained and shows a polygonal texture. Biotite occurs as flakes exhibiting the typical biotite pleochroism. Titanite occurs as irregular aggregates of very fine grains, generally associated with ferromagnesian minerals. Opaque minerals occur as grains with irregular faces commonly associated with the ferromagnesian minerals and titanite which they locally replace.

9.3.1 Interpretation of Petrography

The mineralogy of the samples analysed is typical of mafic rocks (Fig. 9.6).
The mineralogy of samples taken in the west consists of plagioclase±clinopyroxene±amphibole (actinolite)±chlorite±epidote±titanite. This assemblage is typical of basic rocks which have been subjected to low grade metamorphism (Bucher and Frey, 1994, p. 263, 273) (Fig. 9.6.II). In contrast the samples taken further east are characterised by the absence of epidote and actinolite and the presence

of garnet and in some samples, orthopyroxene. The resultant mineral assemblage is typical of basic rocks that have been subjected to medium- to high-grade metamorphism (Bucher and Frey, 1994, p. 263, 278-279) (Fig. 9.6). The occurrence of the common granoblastic texture suggests that the rocks have been recrystallized which is consistent with the medium grade metamorphism.

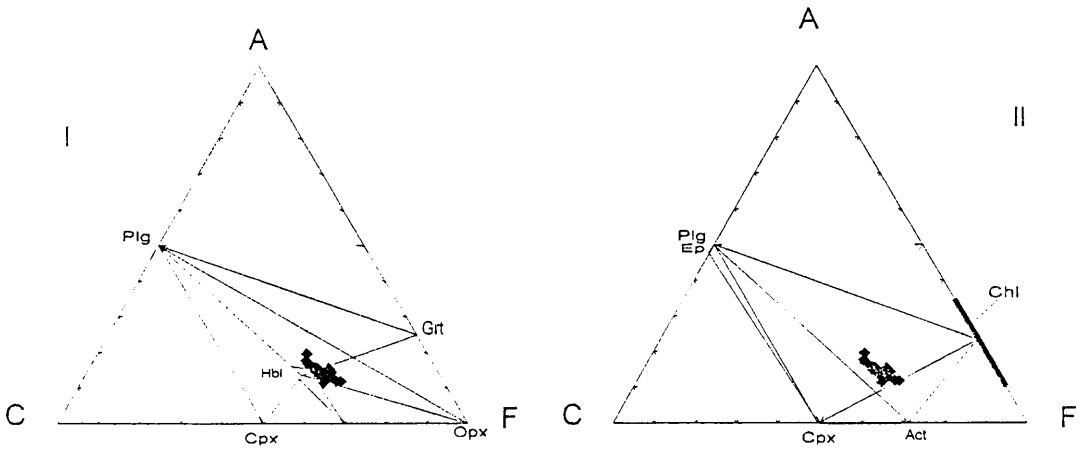

Figure 9.6: ACF diagrams plotting the chemistry and mineralogical assemblages of mafic intrusions. The plotted chemistry is the same in both diagrams. The diagram I shows the mineralogy of high grade metamorphic rocks from the east whereas the diagram II shows mineralogy of the mafic rocks with igneous texture from west.

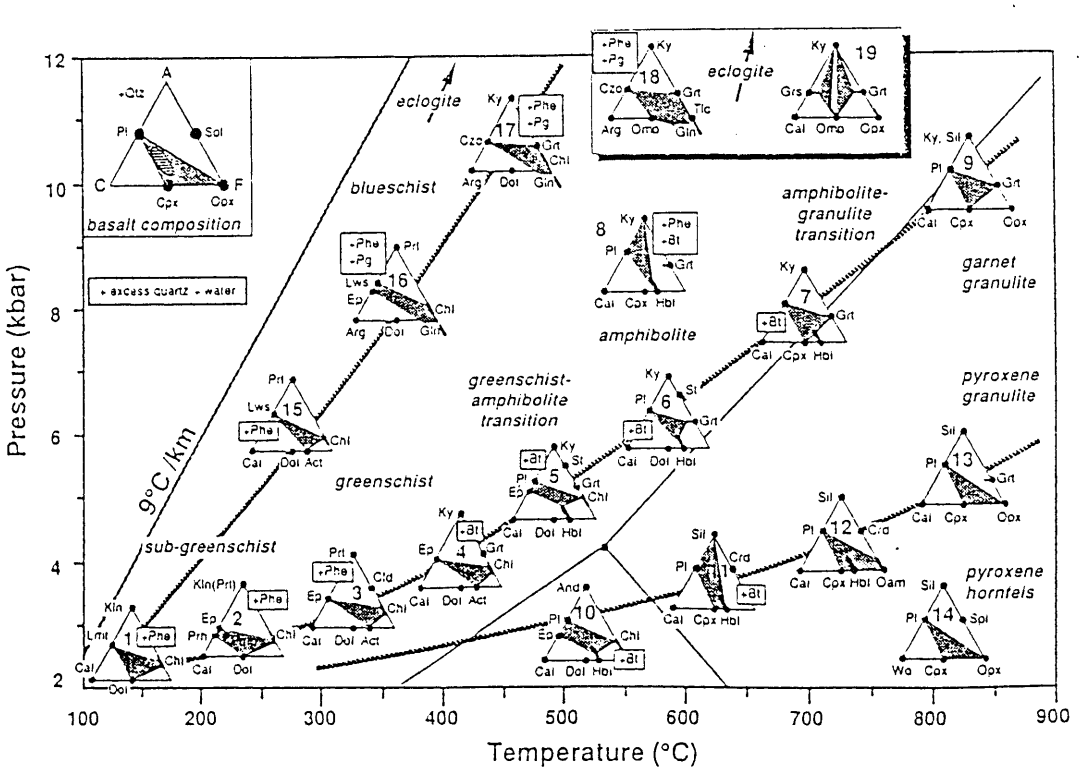

Figure 9.7: Metamorphism of basic rocks represented by the chemographies which are presented as ACF diagrams (after Bucher and Frey, 1994).

Comparing the assemblages of the samples with those from Figure 9.7, it can be seen that the metamorphic grade in the samples increases from chemography 5 (Fig.9.7) in the west, through chemography 6, 7 to one intermediate between chemographies 9 and 13 in the east. The latter chemographies are consistent with the partial melting of a mafic dyke in the east (Figure 9.1). The variation in P-T between chemographies 5 and a point between chemographies 9 and 13 suggests an increase in T from W to E of ~500 °C to ~750 to 800 °C and an increase in P of ~5 to 8 kbar and hence a metamorphic gradient of ~30 °C/Km.

9.4 Chemistry

The geochemical data discussed here are derived from the present study as well as from Manuel (1992). Most of the rocks from Manuel (1992) were described by him as metabasites. The chemical composition of all samples is shown on Table 9.2.

Table 9.2: Chemical composition of mafic intrusions.

SAMP	15M	12T	MDO	18S	MAMP2	MAAMP	MAMP1	99	116	58	158	144	39	233	23	239	38	93	129	6	2
SiO_2	48.89	48.81	48.88	49.44	49.24	50.03	49.16	50.65	51.1	48.08	48.08	50.6	55.46	49.26	51.53	51.46	54.06	50.95	51.59	50.3	50.8
A_2O_3	12.92	15.08	14.07	12.99	13.5	11.69	13.57	13.99	13.66	12.64	14.46	13.81	14.48	12.46	13.52	13.06	14.48	14.06	12.76	13.72	13.2
Fe_2O_3	5.61	5.50	3.26	3.94	3.64	3.87	4.12	4.64	6.19	5.65	4.16	5.52	3.81	6.28	6.13	5.22	3.86	4.29	5.11	4.72	6.0
FeO	12.44	11.79	9.18	10.14	10.19	11.09	11.25	9.33	10.50	10.89	8.29	9.70	6.92	11.38	10.46	9.93	6.75	8.37	10.23	9.22	10.2
MgO	4.69	3.55	8.37	6.65	9.04	8.74	7.66	5.27	3.98	5.34	5.85	4.52	5.83	5.21	3.97	5.92	5.91	7.06	5.49	6.56	3.9
CaO	8.45	8.45	11.02	10.4	10.83	11.87	10.35	10.69	8.26	9.59	10.29	9.41	9.48	8.96	8.26	10.07	9.71	10.56	10.62	9.07	8.6
Na_2O	2.85	3.08	1.68	2.55	2.01	1.86	2.28	2.06	2.69	2.38	2.26	2.55	1.18	2.56	2.62	2.18	1.86	2.19	1.96	2.46	2.6
K_2O	1.31	1.36	0.67	0.44	0.37	0.3	0.29	0.18	1.22	0.78	0.55	1.08	1.19	1.02	1.16	0.48	1.16	0.31	0.15	0.15	1.3
TiO_2	2.24	2.43	0.85	1.81	1.09	1.16	1.3	1.48	2.11	3.16	1.64	1.8	0.77	2.2	2.15	1.31	0.76	1.04	1.36	1.57	2.0
P_2O_5	0.31	0.3	0.06	0.21	0.22	0.08	0.11	0.16	0.26	0.31	0.17	0.22	0.08	0.2	0.22	0.11	0.09	0.09	0.11	0.13	0.2
MnO	0.23	0.22	0.2	0.2	0.22	0.21	0.2	0.2	0.22	0.22	0.19	0.21	0.17	0.24	0.2	0.22	0.17	0.19	0.23	0.19	0.2
total	**99.94**	**100.57**	**98.24**	**98.77**	**100.35**	**100.9**	**100.29**	**98.65**	**100.19**	**99.04**	**95.94**	**99.42**	**99.37**	**99.77**	**100.22**	**99.96**	**98.81**	**99.11**	**99.61**	**98.09**	**99.6**
Ba	335	330	92	154	80	119	139	41	375	186	140	347	344	4	316	99	278	75	43	42	20
Co	63	61	82	66	64	93	86	50	50	60	43	42	40	51	50	48	41	146	43	44	5
Cr	43	44	359	72	272	155	87	80	60	100	100	110	40	70	30	130	50	270	100	150	3
Cu	265	342	94	89	151	169	194	97	246	157	83	266	73	262	219	106	63	77	76	38	17
Nb	13	13	4	11	5	4.4	4.7	5	10	14	8	9	6	9	9	5	7	5	6	8	
Ni	54	45	149	65	141	131	122	88	46	79	64	57	74	59	50	66	73	111	52	67	5
Sc	38	32	44	38	45	51	42	0	0	0	0	0	0	0	0	0	0	0	0	0	
Sr	139	170	94	224	118	112	132	105	142	241	218	140	121	131	155	93	120	95	86	114	15
Rb	46	46	32	12	14	8.5	11	9	46	23	17	40	49	44	75	20	51	19	5	4	7
V	431	568	275	319	303	376	335	340	390	430	280	340	210	490	430	320	190	260	300	330	41
Y	55	52	21	30	25	23	25	28	50	37	22	48	22	36	35	26	21	21	28	36	3
Zn	148	149	5.3	104	98	95	102	95	129	143	88	102	77	112	121	109	76	90	106	112	13
Ga	22	26	15	19	16	18	19	0	0	0	0	0	0	0	0	0	0	0	0	0	
Zr	217	244	54	135	75	70	81	90	195	190	107	159	106	146	164	84	109	72	92	119	14

Samples numbered without letters are from Manuel (1992).

Most of samples are characterized by typical basaltic silica contents, are relatively rich in Al_2O_3 and show a large variation of iron, MgO and TiO_2 contents. Plot of FeO and TiO_2 show linear trends with negative slopes resulting from these elements increasing in relation to decreasing MgO contents (Fig. 9.8). CaO increases sympathetically with MgO suggesting that clinopyroxene fractionation has controlled the CaO/MgO variation. This suggestion is consistent with the clinopyroxene being the dominant pyroxene in the rock samples, particularly those with more or less pristine igneous mineral assemblages.

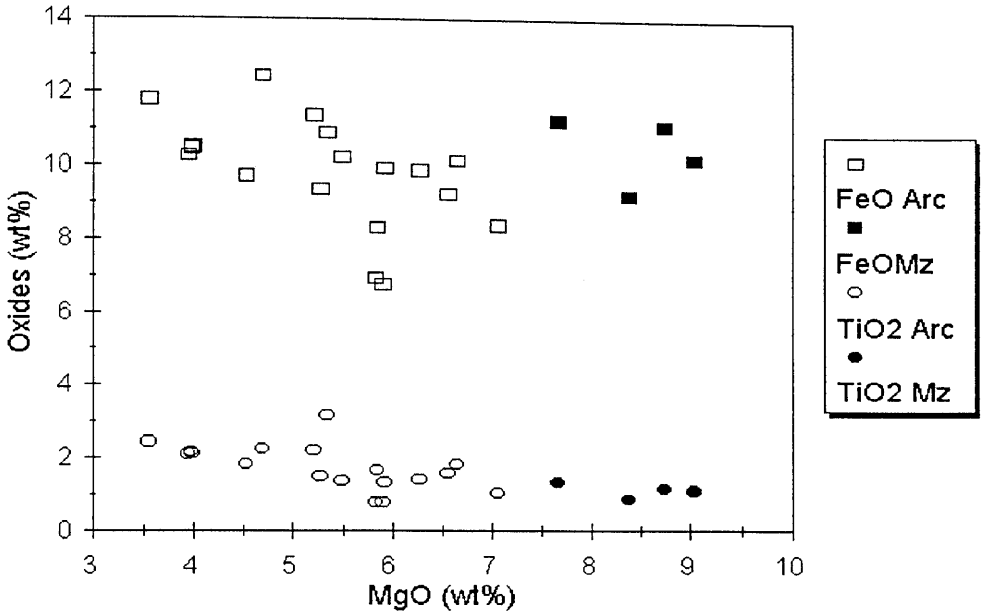

Figure 9.8: Harker diagram of FeO and TiO_2 versus MgO of Mafic intrusions . Mz- samples from Mozambique Belt and Arc- samples from Archaean Granite-Greenstone Belt.

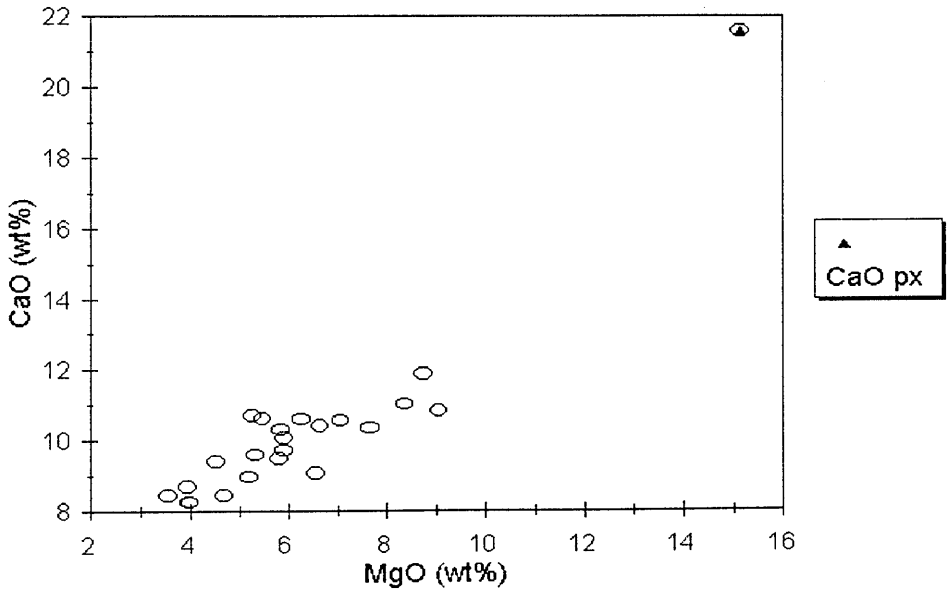

Figure 9.9 CaO versus MgO variation diagram of mafic intrusions. Shown in the diagram is the plot of chemical data of an augite (px) from Deer, Howie and Zussman (1992) (analysis No 8).

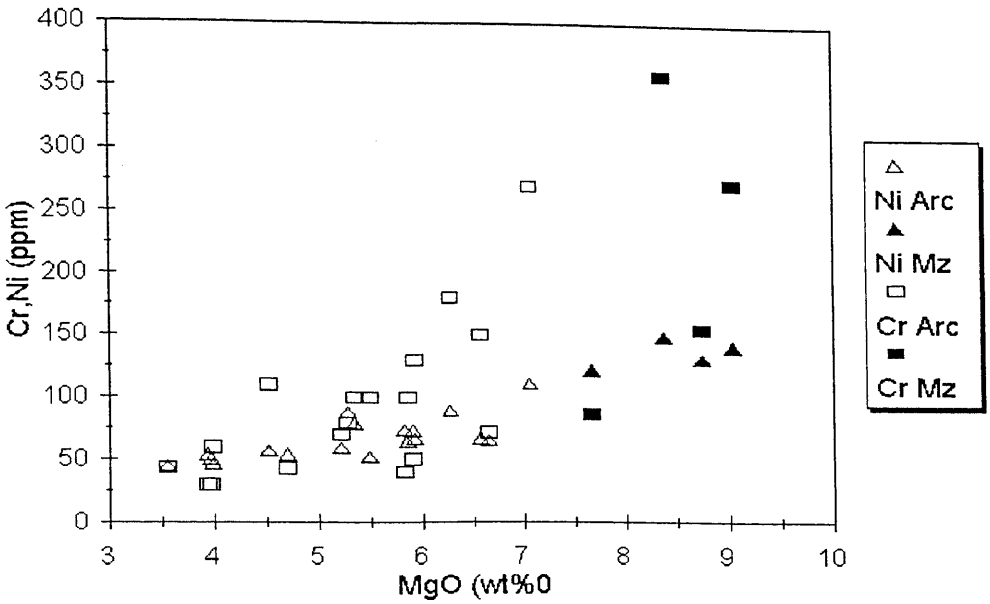

Figure 9.10: Harker diagram plotting Cr and Ni versus MgO of Mafic Intrusions. Abbreviations as in Figure 9.8.

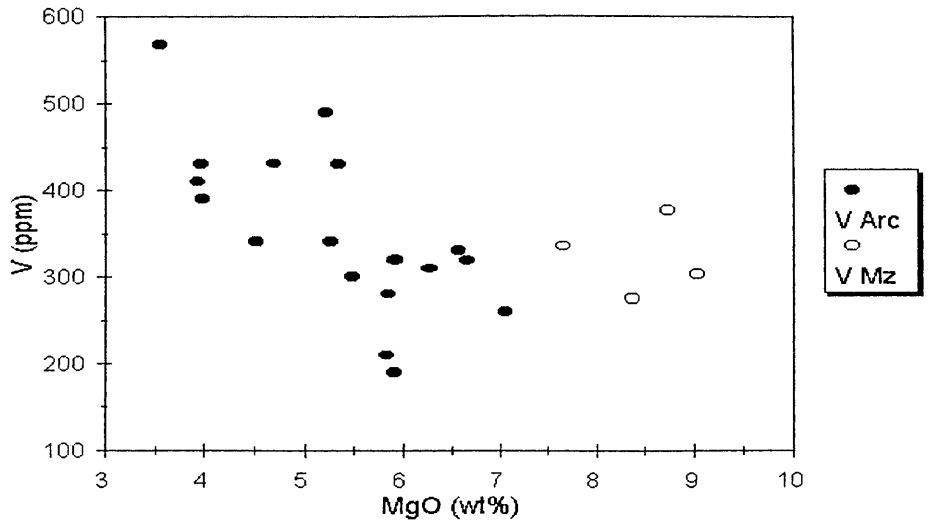

Figure 9.11: Harker diagram plotting V versus MgO of Mafic Intrusions. Abbreviations as in Figure 9.8.

The analyses of an augite from Deer, Howie and Zussman (1992, p. 229) supports this assessment as it plots along the CaO versus MgO trend (Fig. 9.9). Figure 9.10 shows linear variations between Cr and Ni versus MgO. These variations are consistent with clinopyroxene fractionation with both Cr and Ni being strongly fractionated into clinopyroxene (Rollinson, 1993). An inverse correlation between V and MgO is seen (Fig. 9.11), similar to that seen for TiO_2 and FeO versus MgO. These similarities suggest that fractionation of ilmenite and or magnetite have contributed to this variation as these elements are necessary components of these minerals (Rollinson, 1993).

9.4.1 Interpretation of Chemistry

Jensen (1976) described a ternary discriminant diagram to classify rocks ranging from acid volcanics to peridotitic komatiites. In the field of tholeiites, he discriminated between high iron (HFT) and high magnesium (HMT) tholleiites. The samples from the mafic intrusions are all tholeiites and plot mostly in the HFT and a few in the HMT fields (Fig.9.12). Figures 9.13 and 9.14 (Irvine and Baragar,1971) suggest that the mafic intrusions are dominantly sub-alkaline and tholeiites respectively.

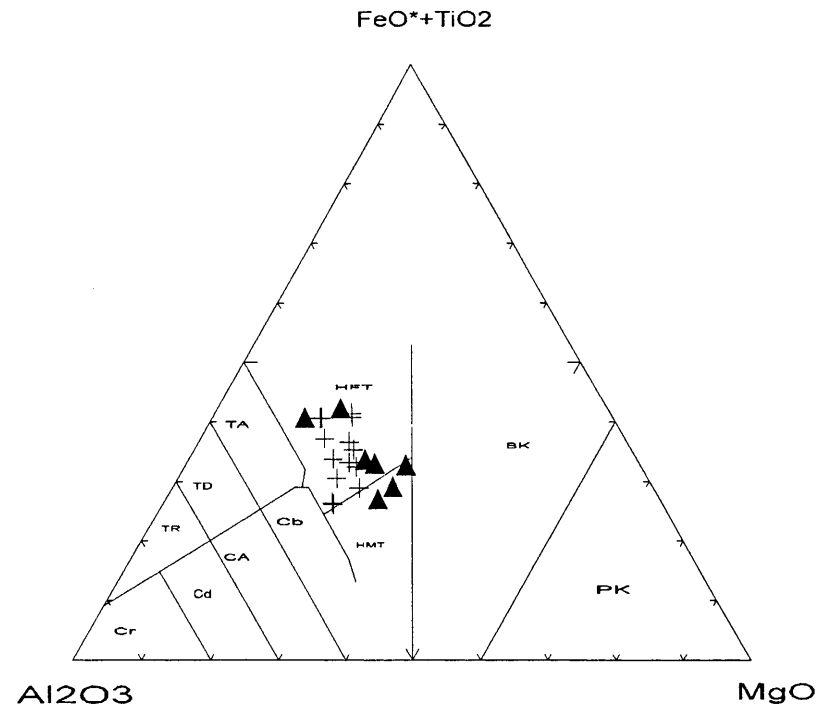

Figure 9.12: Jensen (1976) discriminant diagram plotting chemical data in the fields of high iron (HFT) and high magnesium (HMT) tholeiite fields. Filled up triangles data from Manuel (1992) and crosses, present study. HF- high iron tholeiites, HM- high magnesium tholeiites, BK- basaltic komatiites, PK- peridotitic komatiites, TR- tholeiitic rhyolites, TD- tholeiitic dacites, TA- tholeiitic andesites, CR- calc-alkaline rhyolites, CD- calc-alkaline dacites, CA- calc-alkaline andesites and CB- calc-alkaline basalts.

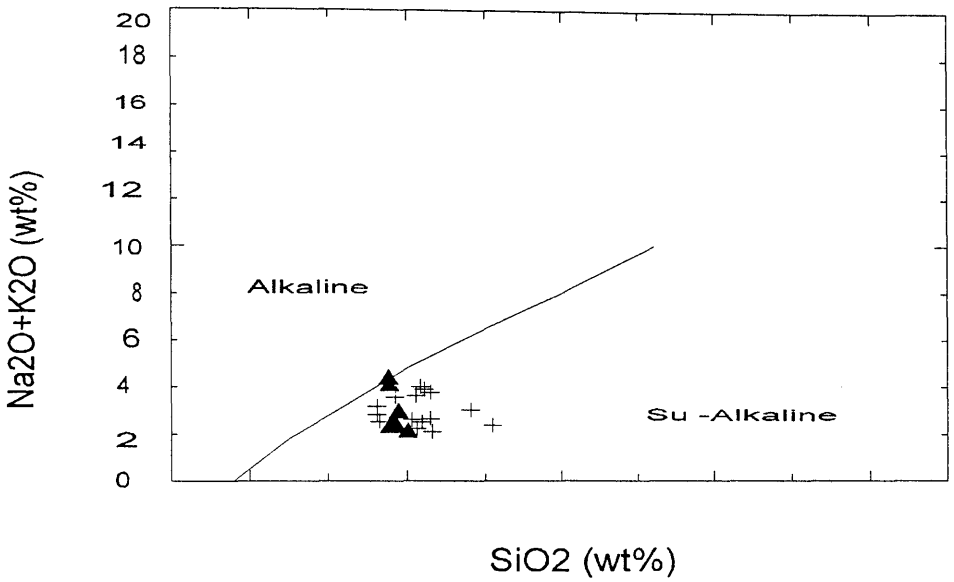

Figure 9.13: Chemical data of mafic intrusions plotting as mostly sub-alkaline (Irvine and Baragar, 1971). Filled up triangles- present study and crosses- Manuel (1992).

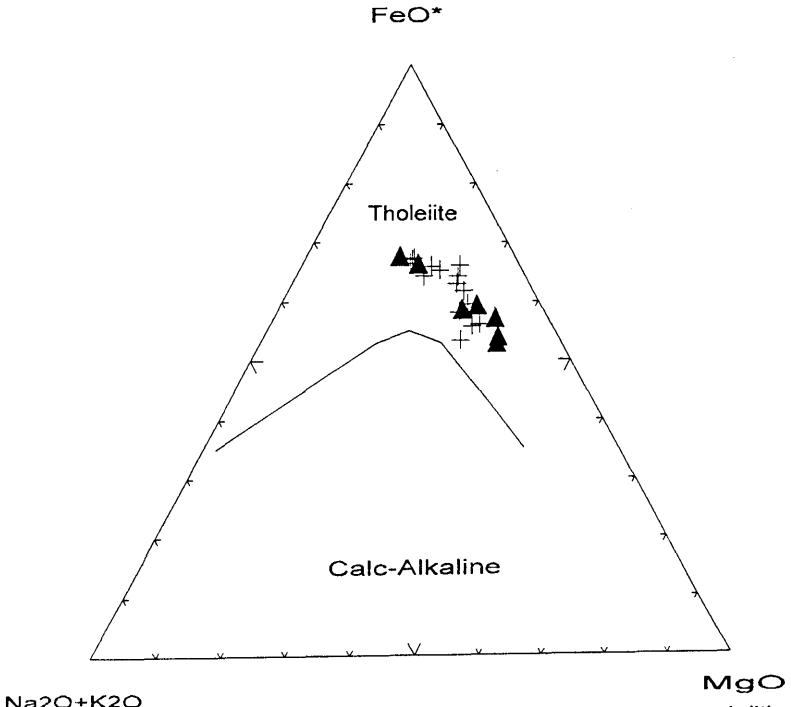

Figure 9.14: Chemical data of Mafic Intrusions indicate a tholeiitic composition in the Irvine and Baragar (1971) discriminant diagram. Symbols as in Figure 9.13.

The analyses of samples 15M and 12T, with igneous textures, Maamp and Maamp2, with metamorphic textures, and 158 and 144 from Manuel (1992) were selected and plotted as spider diagrams (Figs. 9.14 and 9.15). In Figure 9.15 the data are normalized to MORB using values from Pearce (1983) whereas in Figure 9.16 are chondrite normalized using values from Sun (1980). For each diagram it is observed that the samples have similar trends with both diagrams suggesting that their values are 10-100 times higher than those of MORB and chondrites. The trends in these diagrams are similar to those of Pearce (1983) and Sun (1980) respectively for island-arc tholeiitic basalts and are in agreement with Wood (1979) who suggested that in basalts, enrichment in Rb, Ba and K and depletion in Nb is characteristic of island-arc tholeiitic basalts.

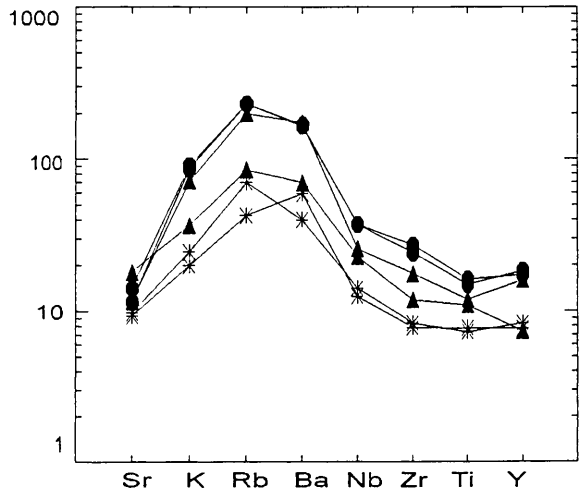

Figure 9.15: MORB normalized trace elements abundance variation diagram. Normalizing data from Pearce (1983). Circles- samples with igneous textures, asterix- samples with metamorphic textures and triangles- analyses from Manuel (1992).

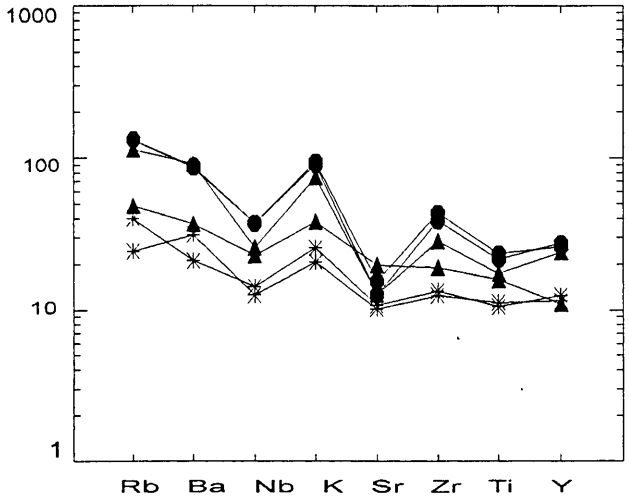

Figure 9.16: Chondrite normalized trace elements abundance variation diagram. Normalizing data from Sun (1980). Circles- samples with igneous textures, asterix- samples with metamorphic textures and triangles- analyses from Manuel (1992).

In conclusion the mafic intrusions comprise two coeval categories of rocks, namely, one occurring within the granite - greenstone belt and characterized by igneous texture and metamorphosed to low grade greenschist facies and another which includes the rocks occurring as dykes within the Mozambique Metamorphic Province and metamorphosed to medium to high grade amphibolite facies. Both rocks have an island-arc tholeiite chemical signature.